D-MESON NUCLEAR MODIFICATION FACTOR IN Pb–Pb COLLISIONS MEASURED WITH ALICE*

Cristina Bedda

for the ALICE Collaboration

INFN and Polytechnic of Turin
Corso Duca degli Abruzzi, 24 — 10129 Turin, Italy

(Received April 28, 2014)

The ALICE results on open heavy-flavour production in pp, p–Pb and Pb–Pb collisions are presented, focusing on the D^0, D^+, D^{*+} and D_s^+ meson nuclear modification factors (R_{AA} and $R_{p\mathrm{Pb}}$). The results obtained from Pb–Pb collisions at $\sqrt{s_{NN}} = 2.76$ TeV collected in 2011 indicate a strong suppression of the D-meson yield at intermediate/high p_{T} in central collisions. The comparison to results in p–Pb collisions suggests that this suppression is a final-state effect due to the presence of the hot and dense medium created in heavy-ion collisions at the LHC.

DOI:10.5506/APhysPolB.45.1281
PACS numbers: 14.40.Lb, 13.25.Ft

1. Heavy quarks: physics motivations

The aim of the ALICE experiment at the LHC is to study the behaviour of strongly interacting matter at very high temperatures and energy densities, as can be created in central Pb–Pb collisions at ultrarelativistic energies.

Heavy quarks (charm and beauty) can be used to study the properties of such matter since they are produced in parton scattering processes with high momentum transfer in the initial stages of the collisions. Therefore, they pass through all the phases of the system evolution losing energy via gluon radiation and elastic collisions in the medium. Heavy quarks give us different information in each type of collisions: in pp their production can be used to test perturbative QCD calculations, in p–Pb they provide an access to cold nuclear matter effects, while in Pb–Pb they are effective probes of the hot and dense QCD medium formed in such collisions.

* Presented at the Cracow Epiphany Conference on the Physics at the LHC, Kraków, Poland, January 8–10, 2014.

Cold nuclear matter effects are a consequence of the presence of a nuclear environment in the initial state of the collision but not of the presence of a deconfined quark–gluon plasma. The initial state effects influence the colliding partons before the hard scattering takes place. One of these effects is the modification of the parton distribution functions in nuclei, which depends on the Bjorken-x and on the nucleus radius/density. In particular, at low Bjorken-x a reduction (called shadowing) of the gluon density in bound nucleons is observed, which is understood as due to gluon saturation at low x. Another effect is the $k_{\rm T}$ broadening that is a consequence of the fact that a parton in a nucleus can undergo multiple elastic scatterings with the partons in the other nucleus before the hard scattering process occurs.

In Pb–Pb collisions, the charm quarks traverse the hot and dense medium interacting with its constituents and losing energy via elastic collisions and gluon radiation. Theoretical models of in-medium energy loss predict a hierarchy in the parton energy loss: $\Delta E_g > \Delta E_{u,d} > \Delta E_c > \Delta E_b$ [1].

With the ALICE apparatus, heavy-flavour hadrons can be detected in various decay channels and in a wide kinematic range. The experimental setup and the strategy followed for these measurements are explained in Sec. 2. D-meson measurements in Pb–Pb collisions at $\sqrt{s_{NN}} = 2.76$ TeV are discussed and compared to other measurements and model calculations in Sec. 3.1. Then, the measurement of the D-meson $R_{p\rm Pb}$ in p–Pb collisions at $\sqrt{s_{NN}} = 5.02$ TeV is shown in Sec. 3.2 and a brief summary is presented in Sec. 4.

2. The ALICE detector and the reconstruction strategy

The ALICE detector [2] consists of a central barrel covering the central rapidity region ($|\eta| < 0.9$) and a muon spectrometer at forward rapidities ($-4.0 < \eta < -2.5$). The detectors of the central barrel are located inside a solenoid magnet delivering a magnetic field of 0.5 T and they allow the reconstruction and identification of charged particles, photons and jets. The central barrel includes the detectors used in the heavy-flavour analyses presented here. The Inner Tracking System (ITS) and the Time Projection Chamber (TPC) provide track reconstruction from ~ 100 MeV/c up to ~ 100 GeV/c transverse momentum with a momentum resolution better than 4% for $p_{\rm T} < 20$ GeV/c. It is possible to obtain an impact parameter (distance of closest approach of the track to the primary interaction vertex) resolution better than 65 μm for $p_{\rm T} > 1$ GeV/c in the bending plane in Pb–Pb collisions. This allows to resolve the decay vertices of D and B mesons, which have decay lengths $c\tau$ of a few hundred μm, making possible the direct reconstruction of charmed hadrons. Charged hadrons are identified using the specific energy deposit (dE/dx) in the TPC and the time-of-flight measured with the Time-Of-Flight (TOF) detector. The VZERO detector, comprising two scintillator arrays located in the forward and backward rapidity regions, is used for fast triggering and for the determination of the event centrality on the basis of the Glauber model.

D^0, D^+ and D^{*+} mesons were reconstructed from their hadronic decays: $D^0 \rightarrow K^-\pi^+$, $D^+ \rightarrow K^-\pi^+\pi^+$, $D^{*+} \rightarrow D^0(\rightarrow K^-\pi^+)\pi^+$, $D_s^+ \rightarrow \phi(\rightarrow K^-K^+)\pi^+$ and their charge conjugates. D-meson candidates are defined from pairs and triplets of tracks with proper charge sign combination and are selected by using a selection based on displaced decay vertex reconstruction and particle identification of the decay tracks. The signal yield is extracted by fitting the invariant mass distributions of the candidates passing these selections. The contribution due to beauty feed-down ($B \rightarrow D$) is subtracted, based on FONLL pQCD calculations and on an assumption on the modification of beauty production in Pb–Pb [3].

3. *D*-meson production in Pb–Pb and *p*–Pb collisions

3.1. Analysis of Pb–Pb collisions at $\sqrt{s_{NN}} = 2.76$ TeV

The reconstruction strategy described in the previous section has been used to analyzed the data sample of Pb–Pb collisions at $\sqrt{s_{NN}} = 2.76$ TeV collected in 2011. The larger statistic in the 2011 Pb–Pb data sample allows to evaluate the D-meson yields in narrower centrality classes and to extend to lower and higher p_{T} the measurements obtained from the 2010 Pb–Pb data sample [4]. The D-meson yields have been measured as a function of p_{T} in a wide momentum range in the most central events (0–7.5%) and as a function of centrality for four different p_{T} intervals. The relative production of D mesons in heavy-ion collisions is compared to pp collisions through the nuclear modification factor R_{AA}, defined as

$$R_{AA} = \frac{dN_{AA}/dp_{\mathrm{T}}}{\langle T_{AA}\rangle d\sigma_{pp}/dp_{\mathrm{T}}}\,, \tag{3.1}$$

where dN_{AA}/dp_{T} is the D-meson yield in Pb–Pb collisions and $d\sigma_{pp}/dp_{\mathrm{T}}$ is the p_{T}-differential cross section of D-meson production in pp collisions and $\langle T_{AA}\rangle$ [1] is the average nuclear overlap function. Because of the limited statistics of the pp data sample collected at $\sqrt{s} = 2.76$ TeV [5], the pp reference is obtained by a pQCD-driven $\sqrt{s}$-scaling of the pp cross section measured at $\sqrt{s} = 7$ TeV. The scaling factor is evaluated as the ratio of the FONLL calculations at these two energies, as detailed in [6].

[1] T_{AA} = convolution of the nuclear density profile of the colliding ions evaluated in the Glauber model.

The dependence of the D-meson R_{AA} on $p_{\rm T}$ is shown in Fig. 1 for the 7.5% most central events in the $p_{\rm T}$ range $3 < p_{\rm T} < 36$ GeV/c. The R_{AA} values measured for D^0, D^+, D^{*+} mesons are compatible within uncertainties over the whole $p_{\rm T}$ range. A suppression by a factor of 4–5 in $5 < p_{\rm T} < 15$ GeV/c is observed in the production yield of D^0, D^+, D^{*+}. The first measurement of the D_s^+ R_{AA}, reported in the figure, shows a suppression by a factor of ≈ 4 in $8 < p_{\rm T} < 12$ GeV/c which is compatible with that of non-strange charmed mesons. At lower $p_{\rm T}$, the central values of the D_s^+ R_{AA} are larger than those of non-strange D mesons, although compatible within uncertainties. More statistics is needed to conclude on the expected enhancement of the D_s^+ yield in Pb–Pb collisions relative to non-strange D mesons in the case of charm hadronization via coalescence [7–9].

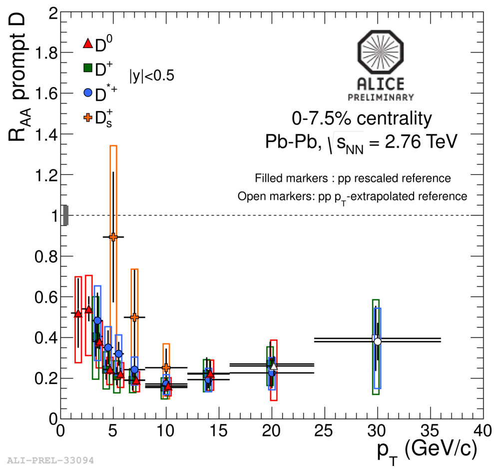

Fig. 1. D^0, D^+, D^{*+}, D_s^+ R_{AA} in the 7.5% most central Pb–Pb collisions as a function of $p_{\rm T}$. Error bars are the statistical uncertainties, empty boxes the total systematic uncertainties.

D-meson production was studied in different centrality classes in the range between 0 and 80%. The centrality dependence of the nuclear modification factor is shown in Fig. 2, for $5 < p_{\rm T} < 8$ GeV/c (left) and for $8 < p_{\rm T} < 16$ GeV/c (right). The centrality ranges considered, 0–10%, 10–20%, 20–30%, 30–40%, 40–50% and 50–80% are reported on the x-axis in terms of the average number of nucleons participating to the collisions, $\langle N_{\rm part}\rangle$, weighted by the number of binary nucleon–nucleon collisions, $N_{\rm coll}$. The suppression of D^0, D^+ and D^{*+} increases with increasing centrality, expressed as the number of nucleons that participate in the collision ($N_{\rm part}$), for both $p_{\rm T}$ ranges.

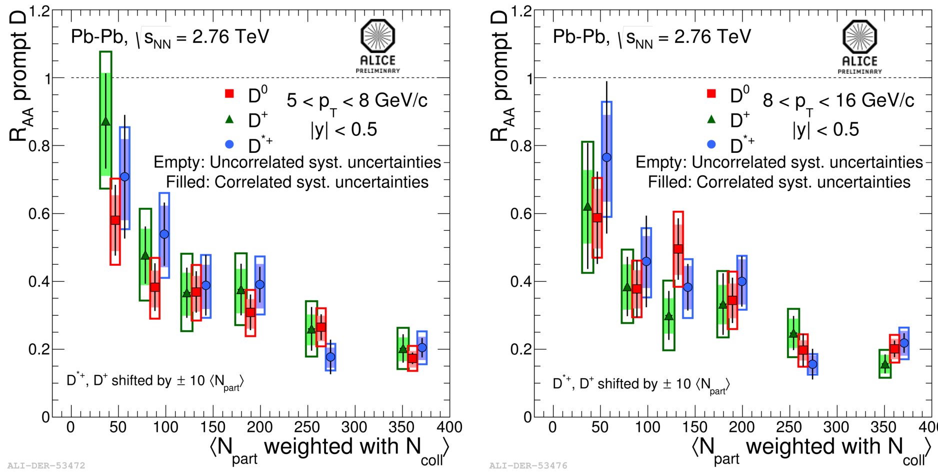

Fig. 2. Comparison of D^0, D^+, D^{*+} R_{AA} *versus* $N_{\rm part}$ in $5 < p_{\rm T} < 8$ GeV/c (left) and in $8 < p_{\rm T} < 16$ GeV/c (right). D^* and D^+ points are shifted by ± 10 in $\langle N_{\rm part} \rangle$ in order to improve the visibility of the individual data plots.

Figure 3 shows the comparison between R_{AA} of prompt D mesons, obtained by averaging the D^0, D^+, D^{*+} results, and the R_{AA} of non-prompt J/ψ, *i.e.* J/ψ from B mesons decays, measured by the CMS Collaboration [10]. The $p_{\rm T}$ ranges were chosen to ensure similar kinematics for D and B mesons. In both $p_{\rm T}$ ranges, a difference between charm and beauty

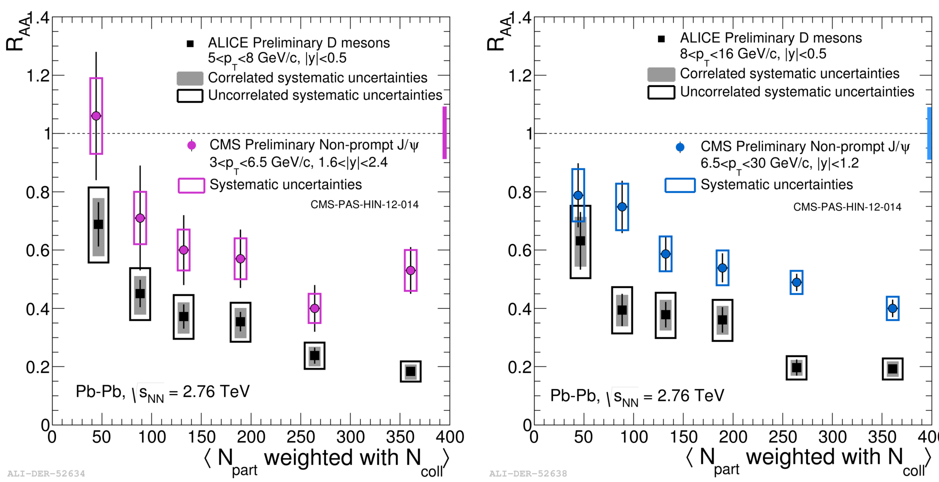

Fig. 3. Comparison of the average D^0, D^+, D^{*+} R_{AA} as a function of $N_{\rm part}$ for $5 < p_{\rm T} < 8$ GeV/c (left) and $8 < p_{\rm T} < 16$ GeV/c (right) to the non-prompt J/ψ for $3 < p_{\rm T} < 6.5$ GeV/c (left) and $6.5 < p_{\rm T} < 30$ GeV/c (right).

suppression in the central and mid-central collisions is observed. The lower R_{AA} of D mesons compared to that of B mesons was predicted in the energy loss models as due to the mass dependence of the medium-induced energy loss.

Figure 4 shows the R_{AA} of D mesons and charged pions as a function of p_{T} in the centrality class 0–7.5% (left) and as a function of the collision centrality for $5 < p_{\mathrm{T}} < 8$ GeV/c (right). The plots show a similar suppression of D mesons and pions but the systematic and statistical uncertainties are too large to draw a conclusion on a potential difference. In addition, the different fragmentation functions of light and heavy quarks make the comparison challenging.

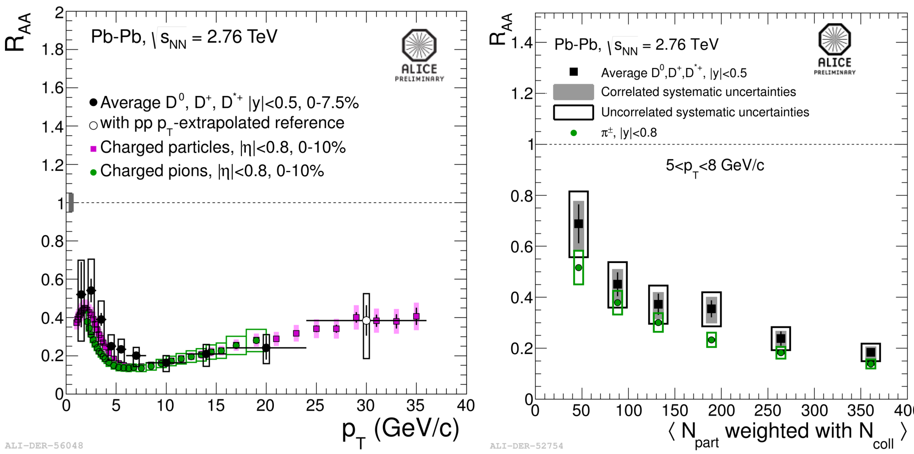

Fig. 4. Comparison of the average D^0, D^+, D^{*+} R_{AA} to the charged pion R_{AA} as a function of the transverse momentum in the most central collisions (0–7.5%) (left) and as a function of the collision centrality for $5 < p_{\mathrm{T}} < 8$ GeV/c (right).

Figure 5 shows the comparison of the average prompt D-meson R_{AA} to several theoretical models based on in-medium parton energy loss [12–17]. All models predict a substantial suppression, while the pQCD calculation with nuclear PDF but without energy loss [11] cannot reproduce the data. In the right panel, models [13, 14, 17] are superimposed to the D meson and non-prompt J/ψ R_{AA} as a function of N_{part} in the p_{T} range of 8–16 GeV/c. All the three models predict a lower R_{AA} of D compared to B mesons.

A reduction of the systematics and statistical uncertainties and new differential measurements will be necessary to disentangle between the different models.

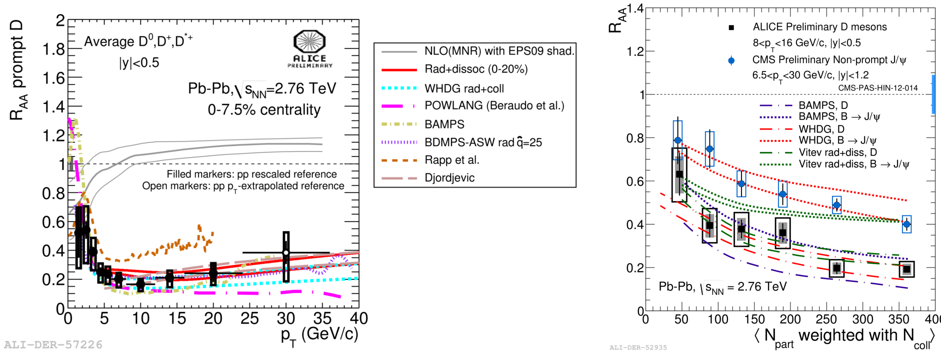

Fig. 5. Prompt D-meson R_{AA} (average of D^0, D^+, D^{*+}) as a function of the transverse momentum in the most central collision 0–7.5% (left) and as a function of the collision centrality in $8 < p_{\mathrm{T}} < 16$ GeV/c (right) compared to NLO MNR calculations with EPS09 shadowing parameterizations [11] and various in-medium energy-loss models: BDMPS-ASW [12], WHDG [13], BAMPS [14], Rapp *et al.* [15], POWLANG [16], Vitev *et al.* [17].

3.2. Analysis of p–Pb collisions at $\sqrt{s_{NN}} = 5.02$ TeV

The study of p–Pb collisions allows us to study cold nuclear matter effects. In p–Pb collisions, the nuclear modification factor $R_{p\mathrm{Pb}}$ is defined as

$$R_{p\mathrm{Pb}} = \frac{1}{A} \frac{d\sigma_{p\mathrm{Pb}}/dp_{\mathrm{T}}}{d\sigma_{pp}/dp_{\mathrm{T}}}\,, \tag{3.2}$$

where A is the atomic mass number of the Pb nucleus, $d\sigma_{p\mathrm{Pb}}/dp_{\mathrm{T}}$ is the p_{T}-differential cross section measured in p–Pb collisions at $\sqrt{s_{NN}} = 5.02$ TeV and $d\sigma_{pp}/dp_{\mathrm{T}}$ is the pp reference, obtained via a pQCD-based scaling of the cross section measured at $\sqrt{s} = 7$ TeV. Figure 6 shows the measured D-meson $R_{p\mathrm{Pb}}$ in p–Pb collisions at $\sqrt{s_{NN}} = 5.02$ TeV. The result is close to unity and it indicates a small nuclear modification in p–Pb collisions of the D-meson production. Perturbative QCD calculations which include the EPS09 parametrization of the nuclear PDFs [11] as well as predictions based on the Colour Glass Condensate model reproduce reasonably well the data.

This result confirms that the suppression observed in central Pb–Pb collisions at high p_{T} is an effect of the hot and dense medium.

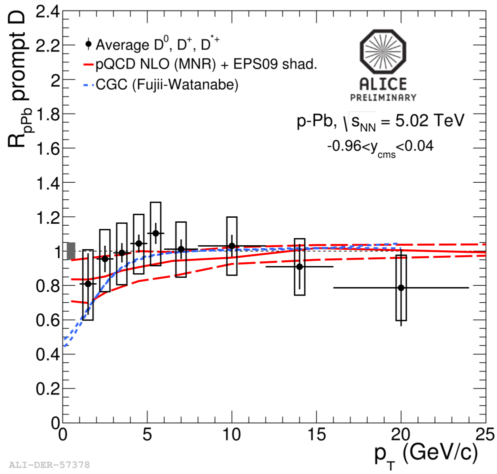

Fig. 6. Comparison of the average D^0, D^+, D^{*+} nuclear modification factor in p–Pb collisions at $\sqrt{s_{NN}} = 5.02$ TeV with the MNR-LO+EPS09 shadowing calculations [11] and the predictions from a Colour Glass Condensate calculation.

4. Summary

D-meson production was studied in pp, p–Pb and Pb–Pb collisions with the ALICE detector at the LHC, and the nuclear modification factors R_{AA} and $R_{p\mathrm{Pb}}$ were reported.

The dependence of the D-meson R_{AA} on the centrality of the collisions and on the transverse momentum of the D mesons has been discussed. The results, obtained from Pb–Pb collisions at $\sqrt{s_{NN}} = 2.76$ TeV collected in 2011, indicate a strong suppression up to a factor of 5 of D^0, D^+ and D^{*+} mesons at intermediate/high p_{T} in central collisions. The first measurement of the D_s^+ meson has also been presented but more statistics is needed to conclude on a possible enhancement of D_s^+ yield relative to non-strange D mesons at low p_{T}. The comparison to the R_{AA} of J/ψ from decays of B mesons (measured by CMS), to that of light hadrons and to various energy-loss models has also been shown. A difference in the D meson and non-prompt J/ψ nuclear modification factors has been observed, as expected from the mass hierarchy in the energy-loss models. The comparison to the $R_{p\mathrm{Pb}}$ demonstrates that the suppression of the D-meson yield at high p_{T} observed in central Pb–Pb collisions is a final-state effect due to the presence of the medium created in heavy-ion collisions at the LHC.

The forthcoming Run 2 will allow to improve our current results increasing the statistics.

REFERENCES

[1] Yu.L. Dokshitzer, D.E. Kharzeev, *Phys. Lett.* **B519**, 199 (2001).

[2] K. Aamodt *et al.* [ALICE Collaboration], *JINST* **3**, S08002 (2008).

[3] M. Cacciari *et al.*, `arXiv:1205.6344 [hep-ph]`.

[4] B. Abelev *et al.* [ALICE Collaboration], *J. High Energy Phys.* **09**, 112 (2012) [`arXiv:1203.2160 [nucl-ex]`].

[5] B. Abelev *et al.* [ALICE Collaboration], *J. High Energy Phys.* **07**, 191 (2012).

[6] B. Abelev *et al.* [ALICE Collaboration], `arXiv:1111.1553 [hep-ex]`.

[7] J. Kuznetsova, J. Rafelski, *Eur. Phys. J.* **C51**, 113 (2007).

[8] M. He, R.J. Fries, R. Rapp, *Phys. Rev. Lett.* **110**, 112301 (2013) [`arXiv:1204.4442 [nucl-th]`].

[9] A. Andronic, P. Braun-Munzinger, K. Redlich, J. Stachel, *Phys. Lett.* **B659**, 149 (2008) [`arXiv:0708.1488 [nucl-th]`].

[10] CMS Collaboration, *J. High Energy Phys.* **05**, 063 (2012) [`arXiv:1201.5069 [nucl-ex]`].

[11] K.J. Eskola, H. Paukkunen, C.A. Salgado, *J. High Energy Phys.* **0904**, 065 (2009).

[12] N. Armesto, A. Dainese, C.A. Salgado, U.A. Wiedemann, *Phys. Rev.* **D71**, 054027 (2005).

[13] W.A. Horowitz, M. Gyulassy, *J. Phys. G* **38**, 124114 (2011).

[14] O. Fochler, J. Uphoff, Z. Xu, C. Greiner, *J. Phys. G* **38**, 124152 (2011).

[15] M. He, R.J. Fries, R. Rapp, *Phys. Rev.* **C86**, 014903 (2012).

[16] W.M. Alberico *et al.*, *Eur. Phys. J.* **C71**, 1666 (2011); *J. Phys. G* **38**, 124144 (2011).

[17] R. Sharma, I. Vitev, B.-W. Zhang, *Phys. Rev.* **C80**, 054902 (2009); *Phys. Lett.* **B713**, 224 (2012).